

## Research Article

# Fucoxanthin-Rich *Padina australis*: Anti-Ageing Properties Through Enzyme Inhibition

Wirasti Wirasti<sup>1,2</sup>, Retno Murwanti<sup>3</sup>, Nanang Fakhrudin<sup>4</sup>, Erna Prawita Setyowati<sup>4\*</sup>

1) Doctor of Pharmaceutical Science Program, Faculty of Pharmacy, Universitas Gadjah Mada, Yogyakarta, Indonesia

2) Pharmacy Undergraduate Study Program, Universitas Muhammadiyah Pekajangan Pekalongan, Jawa Tengah, Indonesia

3) Department of Pharmacology and Clinical Pharmacy, Faculty of Pharmacy, Universitas Gadjah Mada, Yogyakarta, Indonesia

4) Department of Pharmaceutical Biology, Faculty of Pharmacy, Universitas Gadjah Mada, Yogyakarta, Indonesia

\* Corresponding author, email: [erna\\_prawita@ugm.ac.id](mailto:erna_prawita@ugm.ac.id)

### Keywords:

Ageing

Anti-collagenase

Anti-tyrosinase

Brown seaweed

*Padina australis* Hauck

### Submitted:

12 July 2024

### Accepted:

10 September 2025

### Published:

27 March 2026

### Editors:

Ardaning Nuriliani

Sri Nopitasari

### ABSTRACT

The brown seaweed, *Padina australis* Hauck (PAH), known for its high carotenoid content, has been shown to mitigate skin ageing by inhibiting collagenase activity. This study aims to evaluate the inhibitory effects of PAH on collagenase and tyrosinase enzymes. The study begins by extracting the seaweed using ethanol. Afterwards, it is fractionated with ethyl acetate to obtain ethyl acetate-soluble and ethyl acetate-insoluble compounds (EAS and EAI, respectively). The crude extract and both fractions were then subjected to assays to determine their collagenase and tyrosinase inhibitory activities. The results demonstrated that the isolate exhibited the highest inhibition of both enzymes, followed by the EAS, with the EAI showing the least activity. Thin-layer chromatography (TLC) analysis of both fractions revealed retardation factors ( $R_f$  identical) to the standard fucoxanthin. TLC densitometry analysis quantified fucoxanthin concentrations at  $42.36 \pm 3.94 \mu\text{g mg}^{-1}$  in the extract and  $99.104 \pm 7.76 \mu\text{g mg}^{-1}$  in the EAS. Furthermore, the study concluded that the extract, EAS, and isolate had  $IC_{50}$  values below  $100 \mu\text{g mL}^{-1}$ , categorising them as effective inhibitors. The high fucoxanthin content in the extract and fractions suggests significant potential for anti-ageing applications.

Copyright: © 2026, J. Tropical Biodiversity Biotechnology (CC BY-SA 4.0)

### How to cite:

Setyowati, E.P. et al., 2026. Fucoxanthin-Rich *Padina australis*: Anti-Ageing Properties Through Enzyme Inhibition. *Journal of Tropical Biodiversity and Biotechnology*, 11(1), jtbb14712. doi: 10.22146/jtbb.14712

## INTRODUCTION

The global ageing population is rapidly increasing, leading to a higher prevalence of age-related health issues and a growing demand for effective anti-ageing solutions (Tamaz & Nino 2021). This demographic shift is accompanied by an urgent need to address the physiological and cosmetic aspects of ageing, which include skin deterioration, loss of elasticity, and the appearance of wrinkles (Rizzi et al. 2021). The skin, as the body's largest and most visible organ, plays a crucial role in protecting against environmental hazards and regulating body temperature. However, it is also highly vulnerable to the ageing process (Robert et al. 2012). Over time, the structural proteins collagen and elastin, which provide skin with its elasticity and firmness, gradually break down. This degradation leads to the common signs of ageing, such as wrinkles, sagging, and a loss of youthful plumpness (Tzaphlidou 2004). These visible changes are often accompanied by a decrease in the skin's ability to heal and retain moisture, making it more prone to dryness and irritation. Consequently, the quest for effective anti-ageing substances that can mitigate or reverse these effects is a major focus within dermatological research (Park et al. 2014).

Given the urgency to mitigate the effects of ageing, scientific investigations have increasingly focused on natural sources of bioactive compounds that can inhibit enzymes responsible for skin ageing (Mukherjee et al. 2011). Collagenase and tyrosinase are two key enzymes implicated in this process. Collagenase degrades collagen, a protein crucial for maintaining skin structure and firmness, while tyrosinase is involved in melanin production, leading to pigmentation issues (Marques et al. 2021). Additionally, these enzymes, when overactive, can lead to the degradation of essential skin proteins such as collagen and elastin, resulting in premature ageing and other skin issues (Srisuksomwong et al. 2023).

Marine organisms, especially seaweeds, are at the forefront of research for natural inhibitors due to their abundance of bioactive compounds. These compounds have shown potential in protecting against enzyme-related damage, offering a natural solution for skin care (Cao et al. 2020). Seaweeds' unique composition, including antioxidants, peptides, and minerals, contribute to their efficacy in skin preservation (Pangestuti et al. 2021). Since seaweed originates from the ocean, has evolved to withstand extreme conditions, surviving in demanding habitats where it endures powerful waves, high salt concentrations, intense sunlight, and shifting temperatures. To survive, they have evolved protective mechanisms by producing bioactive compounds such as antioxidants, peptides, and polysaccharides. These compounds help seaweeds cope with oxidative stress and environmental damage, and when applied to human skin, they offer similar protective benefits. Antioxidants can neutralise free radicals caused by UV exposure, while peptides and other bioactive molecules support skin regeneration and moisture retention. This resilience, developed in their natural marine habitat, translates into potent protective properties for human skin (Naser 2021), making seaweed-derived ingredients highly effective in skincare formulations. As such, they are increasingly being recognised for their therapeutic benefits and are being incorporated into a variety of skincare products aimed at enhancing skin integrity and appearance (Pereira 2018).

Researchers have taken particular interest in *Padina australis* Hauck (PAH), a brown seaweed, because of its remarkable ability to combat ageing. Among these marine organisms, the brown seaweed, *Padina australis* Hauck (PAH), has garnered attention for its potent anti-ageing properties. PAH is considered superior to other marine organisms due to its rich content of bioactive compounds such as fucoxanthin, phlorotannins, and polysaccharides, which provide potent antioxidants, anti-inflammatory, and anti-ageing prop-

erties. Research shows PAH exhibits strong collagenase and tyrosinase inhibitory activities, essential for skin protection and anti-ageing effects. Moreover, PAH is known to contain high levels of fucoxanthin, a carotenoid with powerful antioxidant capabilities (Thiyagarasaiyar et al. 2021). Fucoxanthin's antioxidant properties are closely associated with its ability to combat oxidative stress, a key factor in the ageing process (Guvatova et al. 2020). By protecting cells from oxidative damage and inhibiting the activity of collagenase and tyrosinase, fucoxanthin helps to maintain skin health and reduce signs of ageing (Chen et al. 2021). This study aims to explore the anti-ageing properties of fucoxanthin-rich PAH through its enzyme inhibition capabilities. By extracting and fractionating the bioactive components of this seaweed, their effectiveness in inhibiting collagenase and tyrosinase was assessed. This study aims to explore PAH's potential as a natural anti-ageing agent, focusing on its ability to inhibit collagenase and tyrosinase, key enzymes linked to skin ageing, to support the development of effective skincare solutions.

## MATERIALS AND METHODS

### Sample Collection

*Padina australis* brown seaweed was collected from the coast of Gunung Kidul, Yogyakarta. The collection was conducted during low tide, typically between 13:00-14:00 and 01:00-03:00. The seaweed was carefully harvested to ensure minimal damage to the samples and the surrounding ecosystem by placing in a covered bucket and promptly transferred it to a sealed cooler to maintain freshness. Upon arrival, it was washed thoroughly under running water to remove impurities, and the roots were discarded to eliminate any sand attached. The seaweed was then drained and immediately dried at a controlled temperature of 50 °C to preserve its quality.

### Methods

#### Extraction and Fractionation

The collected PAH seaweed was thoroughly washed with seawater to remove any attached debris and sand. The cleaned seaweed was then dried at room temperature and ground into a fine powder to create PAH simplicial powder. A total of 500 g of this powdered seaweed was macerated with 3 L of ethanol for three days, with occasional stirring to enhance the extraction process. After the initial 3-day maceration, the seaweed underwent re-maceration with fresh ethanol for an additional three days to ensure maximum extraction of bioactive compounds (Mugiyanto et al. 2019).

The following procedure was adopted from methods previously developed by other researchers, with modifications. The ethanol extract from both maceration phases was then combined, filtered, and concentrated under reduced pressure using a rotary evaporator to obtain the crude extract. Subsequently, fractionation using ethyl acetate (EA) was carried out. The concentrated crude extract was dissolved in ethyl acetate, shaken vigorously, and then separated using a separating funnel, which had been allowed to settle beforehand. The ethyl acetate soluble fraction (EAS) and ethyl acetate insoluble fraction (EAI) were separated accordingly. The EAS and EAI, enriched with targeted bioactive compounds, were further concentrated under reduced pressure to obtain a more refined extract suitable for subsequent assays and analyses (Fajriyah et al. 2024).

#### Fourier Transform Infrared (FTIR) Analysis

For FTIR analysis, the extracted and fractionated samples of PAH were prepared by first drying a small amount of each sample to remove residual solvent. The dried samples were then directly analysed using an FTIR spectrometer. Spectra were recorded over a range of wavelengths typically from

4000 to 400  $\text{cm}^{-1}$ . The FTIR spectra obtained were analysed to identify characteristic absorption bands corresponding to functional groups present in the samples (Waznah et al. 2022).

### Isolation of Active Compounds

Isolation of active compounds from fractions exhibiting collagenase and tyrosinase inhibitory activity was conducted using preparative thin layer (Preparative TLC). Prior to compound separation, the mobile phase selection was crucial and based on solvent polarity, following methods outlined by Nurrochmad et al. (2018). The solvent system employed was methanol: chloroform with varying ratios (80:20 v/v), (60:40 v/v), (50:50 v/v), (40:60 v/v), and (20:80 v/v). Once an optimal mobile phase was determined, preparative TLC was employed to separate compounds. This method was chosen for its simplicity and cost-effectiveness compared to more complex techniques like HPLC or column chromatography. While HPLC might offer better resolution, preparative TLC provided sufficient resolution for the purposes of this study, allowing effective separation of compounds while maintaining practicality and reducing operational costs. The technique was particularly suited to our study's small-scale extraction and isolation objectives, with subsequent analysis confirming the efficacy of the separated compounds (Bhushan 2024; Mondal et al. 2024). Further, separation resulted in distinct bands on the TLC plate, each band was carefully scraped off and subsequently eluted with ethyl acetate. The eluates from each band were concentrated by evaporation to yield isolated compounds. The fucoxanthin isolated in this study was designated as ISO.

### Concentration Analysis

Concentration analysis of the ethyl acetate extract and soluble fraction was performed to quantify the presence of fucoxanthin. Each sample was dissolved in 10 % DMSO to ensure solubility and consistency. A series of concentration standards was prepared for both the samples and the fucoxanthin standard (Sigma Aldrich). For thin-layer chromatography (TLC), 0.2  $\mu\text{L}$  of each prepared sample was applied to a silica gel TLC plate using a Linomat 5 (Camag) applicator. The stationary phase was silica gel GF 60 254 with solvent front position was 90.0mm. The samples were eluted with a solvent mixture of chloroform: ethyl acetate: methanol (5:1:0.5) to separate the components effectively. After elution, the TLC plates were analysed using a Camag densitometer to measure the intensity of fucoxanthin bands (Duraisamy et al. 2023).

### Bioassay for Collagenase Inhibiting Activity

The assessment of collagenase inhibitory activity was conducted using the Collagenase Activity Colorimetric Assay Kit (Sigma Aldrich, MAK 293). To initiate the assay, 10  $\mu\text{L}$  of the sample and 10  $\mu\text{L}$  of collagenase enzyme were combined in each well of a 96-well plate. The volume was then adjusted to 100  $\mu\text{L}$  with assay buffer. Subsequently, 100  $\mu\text{L}$  of substrate solution was added to each well, ensuring thorough homogenization of the contents. The plate was then incubated for a specified duration at 37 °C to allow enzymatic reactions to proceed. Following incubation, the absorbance of the reaction mixture was measured at 405 nm using a microplate reader. This procedure enabled quantification of collagenase activity inhibition by the samples, providing valuable insights into their potential as anti-aging agents (Zhang et al. 2013).

### Bioassay for Tyrosinase Inhibiting Activity

The evaluation of tyrosinase inhibitory activity was performed using the Tyrosinase Inhibitor Screening Kit (Colorimetric, Sigma Aldrich MAK 257). In each well of a microplate, 20  $\mu\text{L}$  of the sample was combined with 50  $\mu\text{L}$  of tyrosinase enzyme solution and 30  $\mu\text{L}$  of tyrosinase substrate. The contents

were thoroughly mixed and incubated for 10 minutes at 25 °C to allow for enzymatic reaction initiation. After the incubation period, the absorbance of the reaction mixture was measured at 510 nm using a microplate reader. Furthermore, for kinetic mode analysis, absorbance measurements were conducted over a period of 60 minutes to monitor the enzymatic reaction progress (Ishihara et al. 2018).

### Data Analysis

The inhibitory activity of the samples against collagenase and tyrosinase enzymes was quantified by determining their IC<sub>50</sub> values, which represent the concentration required to inhibit 50 % of enzyme activity. Each experiment was conducted in triplicate, and the results were expressed as mean ± standard deviation (SD) to ensure reliability and consistency across multiple trials. Furthermore, statistical analysis was performed using SPSS version 2.0 with ANOVA to evaluate the significance of differences between groups. A p-value of less than 0.05 was considered statistically significant, indicating meaningful variations in inhibitory effects among the samples tested (White et al. 2022).

## RESULTS AND DISCUSSION

### Results

#### Characteristics and Harvesting Practices of Wild PAH

PAH specimens were collected from Gunung Kidul Beach, located between coordinates S8°9'2"E110°36'114" and S8°7'5"E110°32'52", during the months of October and November 2023. The collection took place biannually, specifically timed during low tide periods between 13:00-15:00 and 00:00-03:00, to optimise access to the specimens. The ambient seawater salinity was measured at 32.45 - 33.15 ppt. This natural habitat is free from any cultivation by local communities or governmental interventions. Morphologically, *Padina australis* is characterised by its wide, transparent brown thallus, forming sheet-like or filamentous structures, which are typical of this species. Figure 1 illustrates the appearance of the specimens collected in this study.



**Figure 1.** Morphological characteristics of PAH collected from Gunung Kidul Beach, showing its wide, transparent brown thallus structure.

#### Characterization Using FTIR

FTIR analysis was employed to identify functional groups present in the ethyl acetate soluble fraction and isolate of PAH compounds. Spectra were recorded in the range of 4000 to 500 cm<sup>-1</sup>. As depicted in Figure 2, notable differences were observed in the spectral peaks between the fraction and isolate. Specifically, the presence of hydrogen bonds (O-H) was detected at wave-

numbers 3370 and 3384  $\text{cm}^{-1}$ , with a broader peak observed in the isolate between wavenumbers 3200 and 3600  $\text{cm}^{-1}$  compared to the fraction. Hydrocarbon bonds (-C-H) at wavenumber 2922  $\text{cm}^{-1}$  exhibited a sharper peak in the isolate than in the fraction. Additionally, a carbonyl group (C=O) was identified at wavenumber 1718  $\text{cm}^{-1}$ , along with characteristic fingerprint regions between 700-800  $\text{cm}^{-1}$ . Moreover, the functional groups identified in the ethyl acetate-soluble fraction and isolate samples align with previous research findings by Yip et al. (2014), particularly noting typical fucoxanthin compound absorptions in the fingerprint region and an allenic group at wavenumber 1940  $\text{cm}^{-1}$ . Variations in peak intensities between the fraction and isolate suggest the presence of interfering compounds in the fraction, influencing vibrational characteristics of each bond. These bands correspond to common functional groups associated with fucoxanthin and similar carotenoids, reflecting its complex molecular structure.

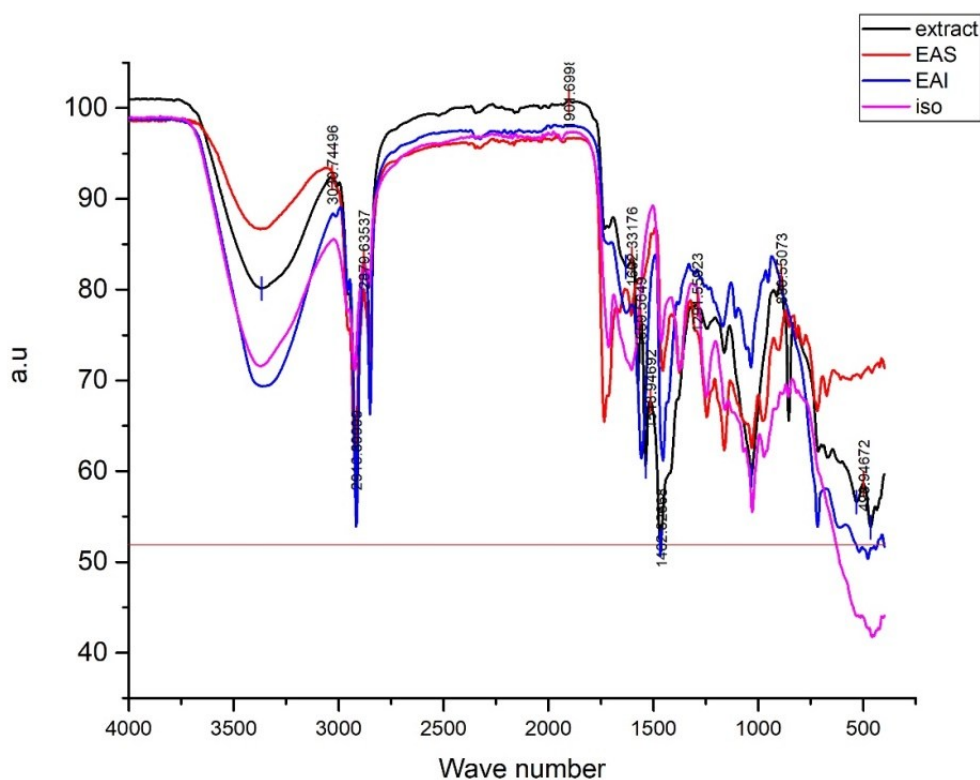


**Figure 2.** FTIR spectra showing characteristic absorption peaks of functional groups in the ethyl acetate: extract, soluble fraction (EAS), insoluble fraction (EAI) and isolate (iso) of PAH compounds.

### Formulation Potential

Before performing densitometric thin-layer chromatography (TLC), the optimisation of the mobile phase was conducted using TLC. The results indicated that the mobile phase (chloroform: ethyl acetate: methanol, 5:1:0.5) provided excellent separation, as evidenced by distinct and well-separated bands. The separated compounds were then subjected to TLC alongside a fucoxanthin standard, with the resulting spot distances corresponding to those of the standard. The outcomes are presented in Figure 3A.

The extract, EAS, and isolate obtained from PAH in this study present promising prospects for further research. To facilitate this process, quantification of active compounds was conducted using TLC-densitometry, focusing on the extract and EAS. Fucoxanthin was employed as the standard chemical for comparative analysis, providing insights into the concentration and distribution of bioactive components within these samples. Figure 3 (B-D) shows the results of TLC-densitometry analysis of the extract and ethyl acetate-

soluble fraction compared with standards. Similar compounds were found between the extract, ethyl acetate-soluble fraction, and fucoxanthin standard at RF 0.8-0.9.

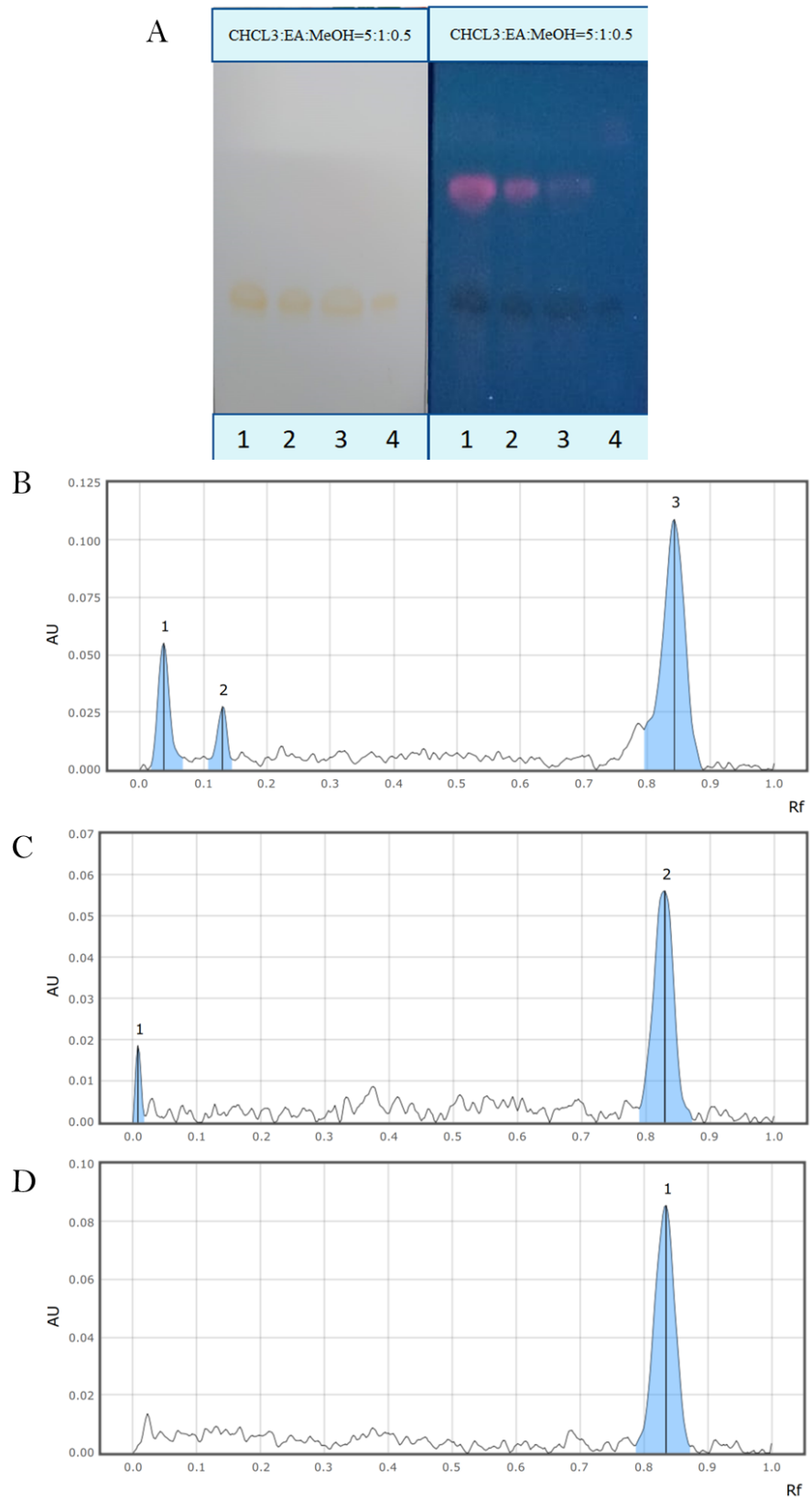


**Figure 3.** The figures represent the results of TLC and TLC-densitometry. (A) shows the TLC outcome using the solvent system chloroform: ethyl acetate: methanol (5:1:0.5), which achieved complete separation. The left panel displays the visualisation under visible light, while the right panel shows the same under UV light. The TLC-densitometry analysis of PAH extract (B), EAS (C), and a standard fucoxanthin from Sigma Aldrich (D) was conducted, with all samples read at a wavelength of 447 nm.

### Quantification of Fucoxanthin Levels

The densitometry analysis conducted in this study provided area under the curve (AUC) data for both the samples and the fucoxanthin standards. A calibration curve was constructed using the AUC data of the fucoxanthin standards, yielding the equation  $Y = 2.516 \times 10^{-8}X + 7.147 \times 10^{-4}$  with an R-squared value of 98.63 % (Figure S1). This calibration curve enabled the quantification of fucoxanthin content in the samples based on their respective AUC values. By applying this curve, the fucoxanthin levels in each replication of the samples could be accurately calculated. The quantification results for the extract and EAS are presented in Figure 4. The fucoxanthin levels were determined to be  $42.36 \pm 3.94 \mu\text{g mg}^{-1}$  and  $99.104 \pm 7.76 \mu\text{g mg}^{-1}$ , respectively, in the extract and EAS.

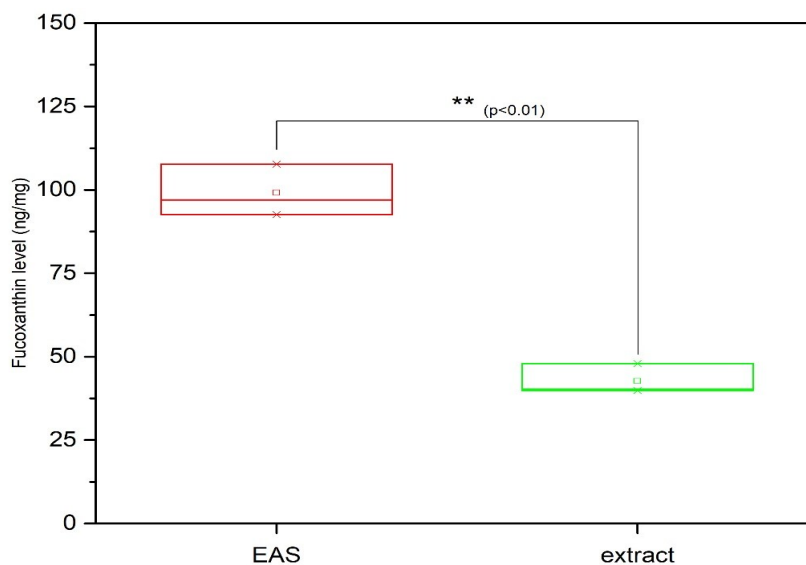


**Figure 4.** Fucoxanthin levels in PAH extract and EAS.

### Collagenase Activity Inhibition

The collagenase activity inhibition assay revealed that the extract, EAS, isolates, and EAI of PAH exhibited varying degrees of inhibitory activity. The assay results, shown in Figure 5A, indicated  $IC_{50}$  values of  $41.96 \pm 2.86 \mu\text{g mL}^{-1}$  for the extract,  $34.57 \pm 0.99 \mu\text{g mL}^{-1}$  for the EA soluble fraction,  $21.78 \pm 1.86 \mu\text{g mL}^{-1}$  for the isolate, and  $-6.30 \mu\text{g mL}^{-1}$  for the EA insoluble fraction. The negative  $IC_{50}$  value of the EA insoluble fraction suggests that the activity of its chemical compounds differs significantly from the other samples. The isolate demonstrated the greatest inhibitory power, which can be attributed to the higher purity of its chemical compounds. This observation is consistent with the  $IC_{50}$  values of the extract and EA soluble fraction, where the fraction with higher inhibitory activity corresponds to a lower  $IC_{50}$  value.

### Tyrosinase Inhibition Activity

The tyrosinase inhibition assay results for the various samples of PAH, including the extract, EAS, EAI, and the isolate, are indicative of their potential anti-tyrosinase activities. The  $IC_{50}$  values, which represent the concentration required to inhibit 50 % of tyrosinase activity, were determined as follows:  $48.42 \mu\text{g mL}^{-1}$  for the extract,  $29.47 \mu\text{g mL}^{-1}$  for EAS,  $11.58 \mu\text{g mL}^{-1}$  for EAI, and  $5.26 \mu\text{g mL}^{-1}$  for isolate (Figure 6B). These findings reveal that the isolate exhibited the highest tyrosinase inhibitory activity with the lowest  $IC_{50}$  value of  $5.26 \mu\text{g mL}^{-1}$ , suggesting that it is the most potent among the tested samples. Furthermore, the progressive increase in potency from the crude extract to the isolate indicates that the active compounds responsible for tyrosinase inhibition are more concentrated in the isolated form. This aligns with the

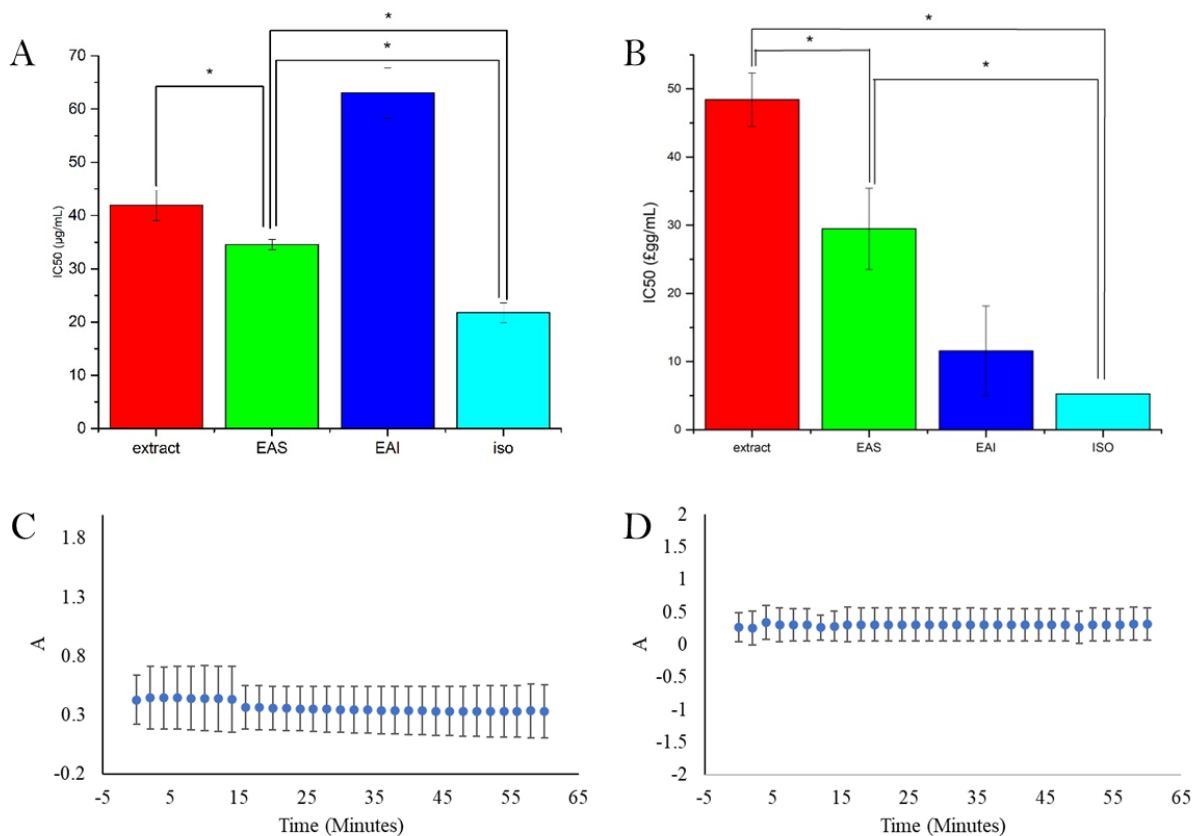


**Figure 5.** The results of the collagenase (A) and tyrosinase (B) inhibition assays were assessed in the extract, EAS, EAI, and isolated compounds (ISO). The effect of DMSO was illustrated in panels (C) and (D) for collagenase and tyrosinase inhibition, respectively, with a significance level of  $p < 0.05$  indicated.

understanding that fractionation and isolation processes effectively enrich the active constituents, such as fucoxanthin, thereby enhancing their bioactivity (Bucar et al. 2013; Wen et al. 2019). These results highlight the potential of PAH as a source of natural tyrosinase inhibitors, which could be developed for anti-hyperpigmentation treatments and other cosmetic applications.

### Discussions

Brown seaweed is composed of a diverse range of bioactive compounds, making it a valuable resource for various applications, particularly in the realm of health and cosmetics (Wang et al. 2020). The primary components include pigments, carbohydrates, phlorotannins, lipids, and low molecular weight organic compounds. The carbohydrate content is notably rich and includes mannitol, fucoidan, alginate, and laminaran. These carbohydrates contribute to the seaweed's structural integrity and offer various health benefits, such as antioxidant and anti-inflammatory properties (Huang et al. 2019). Furthermore, among the pigments, brown seaweed contains a significant amount of carotenoids, a group of pigments responsible for the yellow, orange, and brown colours in many plants. The most prominent carotenoid found in brown seaweed is fucoxanthin as confirmed in our study (Figure 3) (Miyashita et al. 2011).

Antioxidant and anti-inflammatory activities are crucial to anti-ageing, as oxidative stress and chronic inflammation accelerate skin aging. Fucoxanthin's strong antioxidant properties, as shown by Junopia et al. (2020) and Maeda et al. (2018), help prevent oxidative damage, while its anti-inflammatory effects, demonstrated by Zhao et al. (2017), reduce inflammation-related ageing (Zhao et al. 2017; Maeda et al. 2018; Junopia et al. 2020). Together, these properties enhance skin protection, reduce cellular damage, and support fucoxanthin's potential as an effective anti-ageing agent in skin-

care products. In this study, we successfully isolated fucoxanthin from PAH. The confirmation of the isolated fucoxanthin and EAS is evident from the functional group analysis depicted in the Figure 6. The presence of the characteristic allenic bond (C=C=C) in fucoxanthin was confirmed by absorption peaks at  $1930\text{ cm}^{-1}$  and  $929\text{ cm}^{-1}$  in the spectrum, corresponding to the fucoxanthin standard (Yip et al. 2014). Further analysis revealed the absorption peaks at  $3380\text{ cm}^{-1}$  and  $3013\text{ cm}^{-1}$ , indicating the presence of  $\text{-OH}$  bonds, consistent with Purnomo's observations (Zailanie & Purnomo 2011). Additionally, we identified peaks at  $2957\text{ cm}^{-1}$  and  $2855\text{ cm}^{-1}$ , suggesting the presence of alkanes with C-H bonds, further corroborating the structural characteristics of fucoxanthin. Moreover, our results included an absorption peak at  $1732.54\text{ cm}^{-1}$ , which also pointed to the presence of ketones with  $\text{-C=O}$  bonds, a finding that aligns with Purnomo's earlier work (Zailanie & Purnomo 2011). The peaks identified at  $1455\text{ cm}^{-1}$ ,  $1434\text{ cm}^{-1}$ ,  $1378\text{ cm}^{-1}$ , and  $1364\text{ cm}^{-1}$  indicate the presence of scissoring and bending alkanes with  $\text{-C-H}$  bonds, reinforcing the structural integrity of the isolated fucoxanthin and aligning with the previous studies (Yip et al. 2014). A distinctive feature of our study was the confirmation of the characteristic allenic bond (C=C=C) in fucoxanthin, evidenced by absorption peaks at  $1930\text{ cm}^{-1}$  and  $929\text{ cm}^{-1}$ . This specific characteristic was previously unreported in the context of fucoxanthin isolated from PAH, highlighting a potential area for further research into its unique properties.

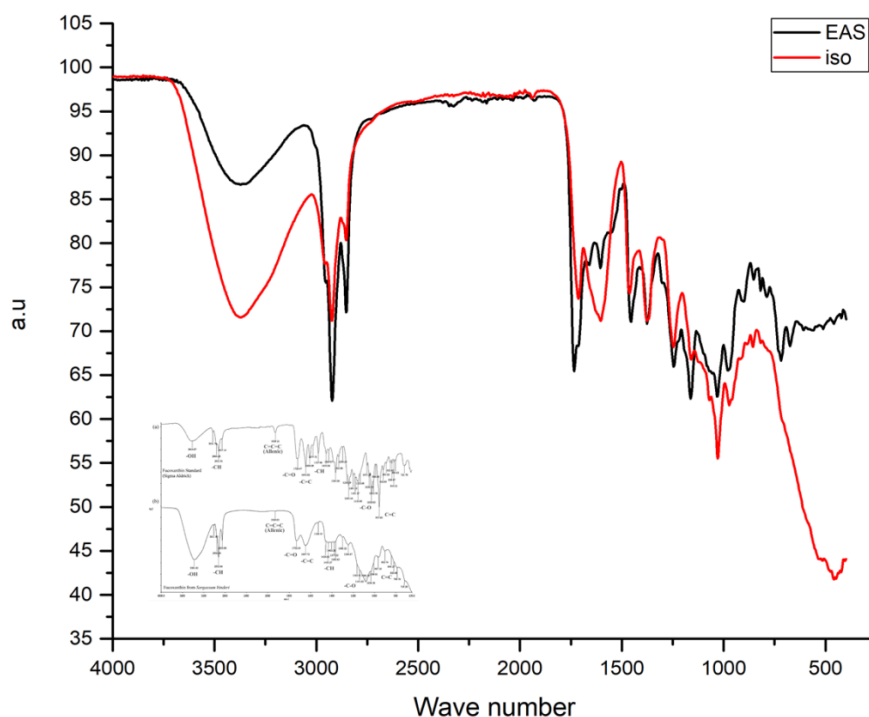


**Figure 6.** FTIR spectra of the EAS and isolate of PAH showing similar characteristic functional groups. Insert is the standard FTIR spectra of fucoxanthin by other study (Yip et al. 2014).

Moreover, the presence of esters with  $\text{-C-O}$  bonds was confirmed by the absorption peak at  $1033\text{ cm}^{-1}$ . These functional groups are characteristic of fucoxanthin. The TLC-densitometry analysis revealed that the fucoxanthin content in the EAS was approximately twice that of the extract (Figure 4). Specifically, the EAS contained  $99.104\text{ }\mu\text{g mg}^{-1}$  of fucoxanthin, compared to  $42.36\text{ }\mu\text{g mg}^{-1}$  in the extract. These results highlight the effectiveness of the ethyl acetate fractionation process in concentrating the bioactive compound, fucoxanthin. This significant increase in fucoxanthin concentration in the EAS underscores its potential for further development. Given the higher pu-

rity and concentration of fucoxanthin, the ethyl acetate soluble fraction exhibits promising potential for use in phytopharmaceutical applications. The enhanced fucoxanthin content in the EAS could lead to more effective formulations for anti-ageing and other health-related products, capitalising on fucoxanthin's well-documented antioxidant and anti-inflammatory properties (Neumann et al. 2019; Bigagli et al. 2021). Moreover, the successful isolation and concentration of fucoxanthin from PAH through ethyl acetate fractionation could streamline the production process in an industrial setting, making it a viable option for large-scale manufacturing of phytopharmaceutical products. This approach not only maximises the yield of the active compound but also enhances the efficacy of the final product, potentially leading to more robust therapeutic outcomes (Atanasov et al. 2015).

Human skin collagenase was initially isolated in active form from skin explant culture medium and subsequently as a proenzyme from monolayer fibroblast cultures. Interstitial collagenase (MMP-1) levels increase with age due to the fragmentation of collagen fibres and disorganisation of the collagen fibre arrangement in the dermis (Nurrochmad et al. 2018). Similarly, tyrosinase is a crucial enzyme in the process of melanogenesis. It contains two copper (II) ions as the main cofactors in the active site, coordinated by six protected histidine residues (Soradech 2016). Our fractionation results demonstrated a significant difference in  $IC_{50}$  values between the EAS and the crude extract, although the EAS still lagged behind the isolated fucoxanthin in terms of inhibitory activity. Specifically, the collagenase inhibition assay revealed that the  $IC_{50}$  values for the EAS were substantially lower than those of the crude extract, indicating a higher concentration of the active compound (fucoxanthin) in the EAS compared to EAI. The higher efficacy of isolated fucoxanthin compared to the EAS and crude extract can be attributed to its greater purity and concentration. Isolated fucoxanthin is present in a purer form, enhancing its bioavailability and interaction with target enzymes like collagenase and tyrosinase (Bucar et al. 2013). In contrast, EAS and crude extracts are complex mixtures that include non-active components which can dilute fucoxanthin's efficacy. The presence of these other compounds may create competitive interactions that reduce fucoxanthin's effectiveness by interfering with its binding to enzyme active sites, resulting in higher  $IC_{50}$  values for the extracts (Atanasov et al. 2015). The isolation process eliminates secondary metabolites that may hinder specific inhibitory activities, allowing the isolated fucoxanthin to exert a more potent effect.

Moreover, the ethyl acetate fractionation process was effective in concentrating fucoxanthin, as evidenced by the lower  $IC_{50}$  values for collagenase inhibition and the higher fucoxanthin content in the EAS. These findings suggest that the EAS is a more potent inhibitor of collagenase and tyrosinase, making it a promising candidate for further development into phytopharmaceutical products aimed at combating skin ageing and hyperpigmentation. This enrichment of fucoxanthin in the EAS highlights its potential utility in anti-ageing formulations, supporting its application in both therapeutic and cosmetic industries. Previous research has shown fucoxanthin inhibits collagenase and elastase, enzymes responsible for the degradation of collagen and elastin, which are essential for maintaining skin elasticity and structure (Freitas et al. 2020; Landa-Cansigno et al. 2023). Additionally, studies have reported its tyrosinase inhibitory activity, which helps in reducing hyperpigmentation by controlling melanin synthesis in the skin (Chen et al 2015; Nurrochmad et al. 2018) These enzyme-inhibitory properties are crucial in delaying skin ageing processes such as wrinkling and age spots. The bioactivity of fucoxanthin, specifically in collagenase and tyrosinase inhibition, aligns with its role in EAS, emphasising its relevance in anti-aging treatments. These findings support its potential application as a key ingredient in cosmeceutical products, driving the development of natural anti-aging solutions based on

seaweed-derived compounds.

## CONCLUSION

This study demonstrates that the EAS fraction and isolated compounds from PAH exhibit significant collagenase ( $IC_{50}$ :  $41.96 \pm 2.86 \mu\text{g mL}^{-1}$  extract,  $21.78 \pm 1.86 \mu\text{g mL}^{-1}$  ISO) and tyrosinase ( $IC_{50}$ :  $5.26 \mu\text{g mL}^{-1}$  ISO) inhibition, highlighting their potential as a natural anti-aging agent. Future research should investigate how environmental factors (e.g., salinity, temperature) affect PAH's bioactive content and whether compound optimisation (e.g., fucoxanthin synergies) could enhance cosmeceutical efficacy, paving the way for pharmaceutical and cosmetic applications.

## AUTHORS CONTRIBUTION

W. designed the study, collected and analysed the data, and wrote the manuscript. R.M. provided consultation on data analysis. N.F. provided consultation on the research process. E.P.S. supervised the entire research process.

## ACKNOWLEDGMENTS

We would like to express our sincere gratitude to the Faculty of Pharmacy at Universitas Gadjah Mada (UGM) for providing the facilities and the funding support (1378/UN1/FA/UP/SK/2024). Additionally, we extend our heartfelt appreciation to Universitas Muhammadiyah Pekajangan Pekalongan (UMPP) for their invaluable support.

## CONFLICT OF INTEREST

The authors declare no conflict of interest.

## REFERENCES

- Atanasov, A. et al., 2015. Discovery and resupply of pharmacologically active plant-derived natural products: A review. *Biotechnology Advances*, 33(8), pp.1582-1624. doi: 10.1016/j.biotechadv.2015.08.001
- Bhushan, R., 2024. Sustainable solutions for direct TLC enantioseparation with in-home thought-out, prepared/modified chiral stationary phases. *Biomedical Chromatography*, 38(12), e6000.
- Bigagli, E. et al., 2021. A Comparative In Vitro Evaluation of the Anti-Inflammatory Effects of a *Tisochrysis lutea* Extract and Fucoxanthin. *Marine Drugs*, 19(6), 334. doi: 10.3390/md19060334.
- Bucar, F., Wube, A. & Schmid, M., 2013. Natural product isolation-how to get from biological material to pure compounds. *Natural Product Reports*, 30(4), pp.525-545. doi: 10.1039/c3np20106f
- Cao, L., 2020. Potential anti-aging substances derived from seaweeds. *Marine Drugs*, 18(11), 564. doi: 10.3390/md18110564.
- Chen, S.-J. et al., 2021. Cytoprotective Potential of Fucoxanthin in Oxidative Stress-Induced Age-Related Macular Degeneration and Retinal Pigment Epithelial Cell Senescence In Vivo and In Vitro. *Marine Drugs*, 19, 114. doi: 10.3390/md19020114
- Chen, W.C. et al., 2015. Discovery of highly potent tyrosinase inhibitor, T1, with significant anti-melanogenesis ability by zebrafish in vivo assay and computational molecular modeling. *Scientific Reports*, 5, 7995. doi: 10.1038/srep07995
- Duraisamy, R. et al., 2023. Method Development And Validation Of Ricinoleic Acid By High Performance Thin Layer Chromatography. *Preprint SSRN*, 4635966.
- Fajriyah, N.N. et al., 2024. Characterization of nano-hydrogel chitosan-annona muricata extract by using ionic gelation. *AIP Conference Proceedings*, 3070, 020008. doi: 10.1063/5.0198874

- Freitas, R. et al., 2020. Highlighting the biological potential of the brown seaweed *Fucus spiralis* for skin applications. *Antioxidants*, 9(7), 611. doi: 10.3390/antiox9070611.
- Guvatova, Z. et al., 2020. Protective effects of carotenoid fucoxanthin in fibroblasts cellular senescence. *Mechanisms of Ageing and Development*, 189(5), 111260. doi: 10.1016/j.mad.2020.111260
- Huang, C., Zhang, Z. & Cui, W., 2019. Marine-derived natural compounds for the treatment of Parkinson's disease. *Marine Drugs*, 17(4), 221. doi: 10.3390/md17040221.
- Ishihara, A. et al., 2018. Novel tyrosinase inhibitors from liquid culture of *Neolentinus lepideus*. *Bioscience, Biotechnology, and Biochemistry*, 82(1), pp.22-30. doi: 10.1080/09168451.2017.1415125
- Junopia, A.C., Natsir, H. & Dali, S., 2020. Effectiveness of Brown Algae (*Padina australis*) Extract as Antioxidant Agent. *Journal of Physics: Conference Series*, 1463, 012012. doi: 10.1088/1742-6596/1463/1/012012
- Landa-Cansigno, C. et al., 2023. The antioxidant and anti-elastase activity of the brown seaweed *Sargassum horridum* (Fucales, Phaeophyceae) and their early phenolics and saponins profiling for green cosmetic applications. *Algal Research*, 75, 103271. doi: 10.1016/j.algal.2023.103271
- Maeda, H. et al., 2018. Anti-oxidant and fucoxanthin contents of brown alga ishimozuku (*Sphaerotrichia divaricata*) from the west coast of aomori, Japan. *Marine Drugs*, 16(8), 255. doi: 10.3390/md16080255
- Marques, R. et al., 2021. Collagenase and Tyrosinase Inhibitory Effect of Isolated Constituents from the Moss *Polytrichum formosum*. *Plants*, 10, 1271. doi: 10.3390/plants10071271
- Miyashita, K., et al. 2011. The allenic carotenoid fucoxanthin, a novel marine nutraceutical from brown seaweeds. *Journal of the Science of Food and Agriculture*, 91(7), pp.1166–1174. doi: 10.1002/jsfa.4353
- Mondal, S. et al., 2024. An overview of extraction, isolation and characterization techniques of phytochemicals from medicinal plants. *Natural Product Research*, pp.1–23. doi: 10.1080/14786419.2024.2426059.
- Mugiyanto, E. et al., 2019. Identifying active compounds of soursop ethanolic fraction as  $\alpha$ -glucosidase inhibitor. *Pharmaciana*, 9, pp.191–200. doi: 10.12928/pharmaciana.v9i2.10105
- Mukherjee, P. et al., 2011. Bioactive compounds from natural resources against skin aging. *Phytotherapy: International Journal of Phytotherapy and Phytopharmacology*, 19, pp.64–73. doi: 10.1016/j.phymed.2011.10.003
- Naser, W., 2021. The Cosmetics Effects of Various Natural Biofunctional Ingredients Against Skin Aging: A Review. *International Journal of Applied Pharmaceutics*, 13(1), pp.10–18. doi: 10.22159/ijap.2021v13i1.39806
- Neumann, U. et al., 2019. Fucoxanthin, a carotenoid derived from *Phaeodactylum tricornerum* exerts antiproliferative and antioxidant activities in vitro. *Antioxidants*, 8(6), 183. doi: 10.3390/antiox8060183
- Nurrochmad, A. et al., 2018. Effects of Antioxidant, Anti-Collagenase, Anti-Elastase, Anti-Tyrosinase of The Extract and Fraction From *Turbinaria decurrens* Bory. *Indonesian Journal of Pharmacy*, 29(4), pp.188-199. doi: 10.14499/indonesianjpharm29iss4pp188
- Pangestuti, R., Shin, K.H. & Kim, S.K., 2021. Anti-photoaging and potential skin health benefits of seaweeds. *Marine Drugs*, 19(3), 172. doi: 10.3390/md19030172.
- Park, S. et al., 2014. Effective Anti-aging Strategies in an Era of Super-aging. *Journal of Menopausal Medicine*, 20, pp.85–89. doi: 10.6118/jmm.2014.20.3.85

- Pereira, L., 2018. Seaweeds as source of bioactive substances and skin care therapy—Cosmeceuticals, algotherapy, and thalassotherapy. *Cosmetics*, 5(4), 68. doi: 10.3390/cosmetics5040068
- Rizzi, V. et al., 2021. Neurocosmetics in skincare—the fascinating world of skin-brain connection: A review to explore ingredients, commercial products for skin aging, and cosmetic regulation. *Cosmetics*, 8(3), 66. doi: 10.3390/cosmetics8030066
- Robert, L., Labat-Robert, J. & Robert, A.-M., 2012. Physiology of Skin Aging. *Clinics in Plastic Surgery*, 39, pp.1–8. doi: 10.1016/j.cps.2011.09.006
- Soradech, S. et al., 2016. Radical scavenging, antioxidant and melanogenesis stimulating activities of different species of rice (*Oryza sativa* L.) extracts. *Thai Journal of Pharmaceutical Sciences (TJPS)*, 40(Supplement Issue), pp.92–95.
- Srisuksomwong, P., Kaenhin, L. & Mungmai, L., 2023. Collagenase and Tyrosinase Inhibitory Activities and Stability of Facial Cream Formulation Containing Cashew Leaf Extract. *Cosmetics*, 10, 17. doi:10.3390/cosmetics10010017
- Tamaz, Z. & Nino, Z., 2021. Population Aging – a Global Challenge. *Ecoforum*, 10(2), 25.
- Thiyagarasaiyar, K. et al., 2021. UVB Radiation Protective Effect of Brown Alga *Padina australis*: A Potential Cosmeceutical Application of Malaysian Seaweed. *Cosmetics*, 8(3), 58.
- Tzaphlidou, M., 2004. The role of collagen and elastin in aged skin: An image processing approach. *Micron*, 35(3), pp.173–177. doi: 10.1016/j.micron.2003.11.003
- Wang, L. et al., 2020. The Potential of Sulfated Polysaccharides Isolated from the Brown Seaweed *Ecklonia maxima* in Cosmetics: Antioxidant, Anti-melanogenesis, and Photoprotective Activities. *Antioxidants*, 9, 724. doi:10.3390/antiox9080724
- Waznah, U. et al., 2022. Comparative Study of FT-IR Profiles Preparation of Nano-Hydrogel Combination of Soursop Extract and Zinc. *Prosiding University Research Colloquium*, pp.286–292.
- Wen, P. et al., 2019. Mulberry: A review of bioactive compounds and advanced processing technology. *Trends in Food Science and Technology*, 83, pp.138–158. doi: 10.1016/j.tifs.2018.11.017
- White, N.M. et al., 2022. An observational analysis of the trope “A p-value of < 0.05 was considered statistically significant” and other cut-and-paste statistical methods. *PloS One*, 17(3), e0264360. doi: 10.1371/journal.pone.0264360.
- Yip, W.H. et al., 2014. Characterisation and stability of pigments extracted from *Sargassum binderi* obtained from Semporna, Sabah. *Sains Malaysiana*, 43(9), pp.1345–1354.
- Zailanie, K. & Purnomo, H., 2011. Studi kandungan dan Identifikasi Fukosantin dari Tiga Jenis Rumpun Laut Cokelat (*Sargassum cinereum*, *Sargassum echinocarpum* dan *Sargassum filipendula*) dari Padike Talogo Sumenep Madura. *Berkala Penelitian Hayati Edisi Khusus*, 7(A), pp.143–147.
- Zhang, Y. et al., 2013. A straightforward ninhydrin-based method for collagenase activity and inhibitor screening of collagenase using spectrophotometry. *Analytical Biochemistry*, 437(1), pp.46–48. doi: 10.1016/j.ab.2013.02.030
- Zhao, D. et al., 2017. Anti-Neuroinflammatory Effects of Fucoxanthin via Inhibition of Akt/NF- $\kappa$ B and MAPKs/AP-1 Pathways and Activation of PKA/CREB Pathway in Lipopolysaccharide-Activated BV-2 Microglial Cells. *Neurochemical Research*, 42(2), pp.667–677. doi: 10.1007/s11064-016-2123-6

## APPENDICES

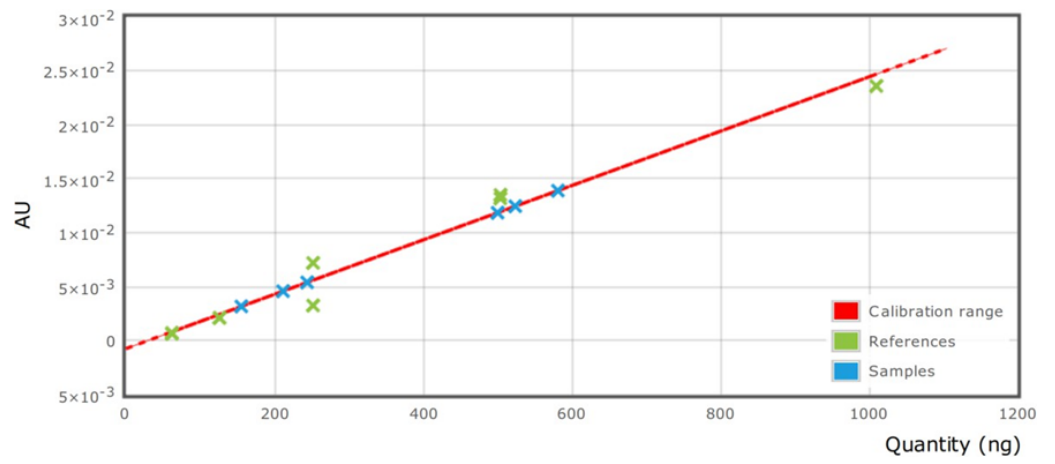


**Figure S1.** Calibration curve of fucoxanthin standard by using CAMAG at 447 nm.